

Low voltage field emission of single Cu nanowire in air with nanoscale gaps for vacuum electronics

Meng Liu^{1,2,3}, Yang Yang^{1,2}, Tie Li^{1,2}, Yuelin Wang^{1,2,3} ✉

¹Science and Technology Lab. on Microsystems, Shanghai Institute of Microsystem and Information Technology, Chinese Academy of Sciences, Shanghai 200050, People's Republic of China

²School of Electronic, Electrical and Communication Engineering, University of Chinese Academy of Sciences, Beijing 100049, People's Republic of China

³School of Information Science and Technology, University of ShanghaiTech, Shanghai 200120, People's Republic of China

✉ E-mail: ylwang@mail.sim.ac.cn

Published in *Micro & Nano Letters*; Received on 9th June 2017; Revised on 17th August 2017; Accepted on 30th August 2017

Field emission applications to date including displays have featured electrode gaps in the micron scale or even larger. Devices such as vacuum field effect transistors demand smaller gaps for improved performance and continued scaling. The present work investigates nanoscale cathode–anode distances and evaluated field emission characteristics using a single Cu emitter. The gap was systematically varied between 20 and 80 nm with the aid of focused ion beam etching. Field emission was achieved at bias voltages below 5 V under atmospheric conditions with a 20 nm gap between the cathode and anode. The turn-on voltage was 1.75 V and the maximum current reached 32.5 nA at 5 V. The emission current is dependent on the cathode–anode distance and decreases exponentially with increasing distance. The nanoscale gap allows lower drive voltages than in previous studies while providing large emission currents for a single emitter.

1. Introduction: Recent advances in nanoelectronics have focused on the construction of field effect transistors using carbon nanotubes, graphene and various group IV and III–V nanowires. However, vacuum as a channel enables higher electron velocity than any of the semiconductor materials in addition to robust operation in high temperature and radiation environments. These advantages have been exploited in recent reports on vacuum field emission transistors (VFETs) fabricated using silicon through a conventional integrated circuit (IC) processing scheme [1–4]. The electrode gap in these studies has been in the nanoscale regime showing significant advantages in terms of drive current, reduction in drive voltage below 10 V and cut-off frequency in the THz range [1]. The use of the IC fabrication scheme also allowed the co-fabrication of a VFET and Metal-Oxide-Semiconductor Field-Effect Transistor (MOSFET) side by side to demonstrate integration capabilities [2] and surround-gate devices [5, 6]. Despite these achievements and the significant advantages that come with the possibility of using the IC infrastructure, silicon may not be the most ideal choice for VFETs from the point of view of work function and robustness. Investigations using alternative materials are needed to advance future developments in this area.

The material history in field emission [7–9] has been dictated by the applications of Spindt cathodes in a wide range of applications including field emission displays, electron sources, microwave devices and sensors. Mo emitters were first reported as field emission cathodes by C.A. Spindt in 1968 [10]. Many metal and semiconductor materials including Si and diamond [11, 12] were used as emitter materials during the next 30 years. Recently, various nanomaterials such as carbon nanotubes [13–15], graphene [16] and SiC [17–19] have been studied to obtain enhanced emission performance by taking advantage of their nanoscale geometry and superior work functions. In addition, different device geometries have also been considered including lateral, vertical, back-gated structures and gate-all-around structures [1, 6, 20, 21] to further reduce the turn-on voltage and gain high current density at sufficiently low voltage.

It is known [15, 22] that a reduction in the cathode–anode distance would enhance the field-emission performance but typically

nanoscale gaps have not been investigated before. Here we have undertaken a study to systematically vary the gap and assess its impact on the emission current. For this purpose, Cu emitters were fabricated by locating a single crystalline Cu nanowire between two electrodes through nanomanipulation, then trimming down the nanowire to the desired thickness and cut off to form a nanogap between the cathode and anode by focused ion beam (FIB) etching. Excellent field emission characteristics in air were realised for these nanoscale gaps with a drive voltage as small as 5 V and an exponential dependence of field emission current on the cathode–anode distance was observed.

2. Experiment: A non-aqueous synthesis method as described in [23] was used to synthesis Cu nanowires. 8 g hexadecylamine and 0.5 g cetyltrimmonium bromide were mixed at 180°C in a glass vial to form a liquid-crystalline medium. 200 mg of copper acetylacetonate were added and stirred for several minutes. Then a silicon wafer covered with platinum film was put into the vial and kept at 180°C for 10 h to form Cu nanowire sheets. Selected-area electron diffraction results (not shown here) confirmed the copper nanowires to be single crystalline. A single nanowire was picked up from the bulk samples using a blunt tungsten probe, placed between the two electrodes and connected to the electrodes by platinum deposition at its ends as shown in Fig. 1. FIB etching was then used to narrow down the nanowire to the desired width. For example, etching for 1 s with FIB working at 30 kV and 1.5 pA allowed reducing the width of the nanowire ~10–14 nm. The nanowire diameter was controlled at ~40 nm by controlling the etch time. Then the nanogap between the cathode and anode was created by cutting off the nanowire as shown in the inset of Fig. 1. For samples with a thickness of ~40 nm, a gap of 20 nm required 300 ms etch time (with FIB working at 30 kV and 1.5 pA) with progressively longer times to create larger gaps. The anode voltage was varied from 0 to 5 V in a Lake Shore Probe Station and the current was recorded by a Keithley 4200-csc Parameter Analyser. All the field emission measurements were performed in air at room temperature (25°C) and 100 kPa for the nanogaps here were much smaller than the

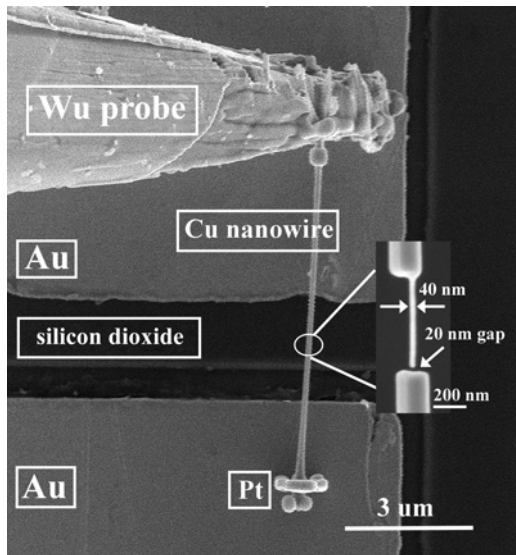


Fig. 1 Scanning electron microscopy (SEM) image of Cu nanowire located between gold electrodes by tungsten probe. The inset shows an SEM image of the Cu nanowire etched and cut off by FIB

mean free path of electrons in air (~ 200 nm) and the applied voltage was not high enough for air molecules to ionise.

3. Results and discussion: The well-known Fowler–Nordheim (F–N) equation is usually used to describe the field emission from metal emitters

$$J = \left(1.54 \times \frac{10^{-6} E_L^2}{\varphi} \right) \exp \left[-6.83 \times \frac{10^7 \varphi^{3/2}}{E_L} \right], \quad (1)$$

where J is the current density (A/cm^2), E is the local electric field (V/cm), and φ is cathode work function (here is 4.5 eV for Cu). Generally, the local field E is related to the applied anode voltage by $E = \beta E_0 = \beta V/d$, where β is the field enhancement factor and $E_0 = V/d$ is the macroscopic applied electric field (d is the distance from the tip of the emitter to the anode).

By replacing J with $J = I/\alpha$ (α is the emitting area) and $E = \beta V/d$, respectively, the F–N equation can also be written as

$$I = A V^2 \exp \left(-\frac{B}{V} \right) \quad (2)$$

$$A = 1.54 \times 10^{-6} \frac{\alpha \beta^2}{\varphi} \quad (3)$$

$$B = 6.83 \times 10^7 \frac{\varphi^{3/2} d}{\beta} \quad (4)$$

Equation (2) is a more practical form of the F–N equation because only the emission current I and applied voltage V can be precisely determined during the field emission measurement. Equation (2) can also be written in logarithm as

$$\ln \left(\frac{I}{V^2} \right) = \ln(A) - B \left(\frac{1}{V} \right) \quad (5)$$

If the carrier transport is dominated by the F–N tunnelling mechanism, the $\ln(I/V^2)$ versus $1/V$ plot (the F–N plot) should show a linear relationship when the applied voltage is big enough. Based on the slope of the F–N plot and (4), the field enhancement factor β can be calculated.

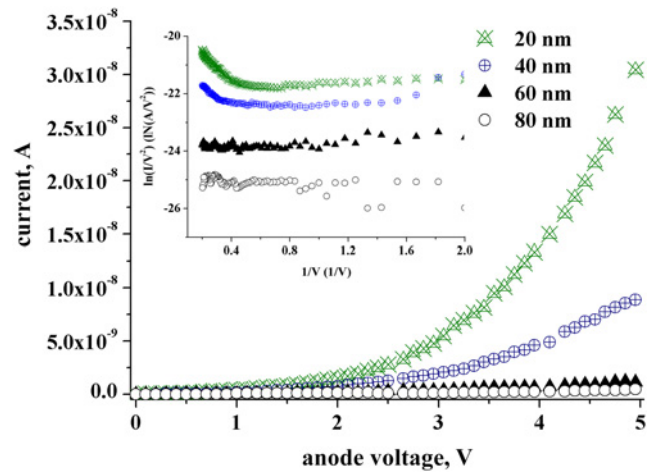


Fig. 2 I – V characteristics of Cu emitters with electrode gaps from 20 to 80 nm. The inset shows the equivalent F–N plots

Fig. 2 shows the emission current for a single Cu tip with different nanogaps in air. For samples with 20 and 40 nm gaps, the emission current increases exponentially with the increase of applied voltage. The turn-on voltage V_{on} (to induce 1 nA) is around 1.75 V and a maximum current of 32.5 nA is achieved at 5 V for emitters with 20 nm gaps. Table 1 compares the performance of recently fabricated field emitters with small gaps described in the open literature. From the table, it can be seen that the V_{on} in our work is the lowest, which is ideal for future Field Emission (FE) based vacuum devices with the potential for scaling. Also the current achieved at 5 V is quite large for a single emitter at such a low applied voltage. In addition, the field emission occurs in air in our work, which is of great importance in terms of reducing the packaging cost. When the nanogap is increased to 40 nm, the corresponding current is much lower than that for emitters with 20 nm gaps. From the inset of Fig. 2, it can be seen that for these two kinds of emitters, there exists a linear relationship between $\ln(I/V^2)$ and $1/V$ when the value of $1/V$ is smaller than about 0.4, which confirms the field emission mechanism during our experiment. The applied voltage here is much lower than that for emitters with a vacuum gap larger than a few hundred microns, usually in the order of 10^2 – 10^4 V. This indicates the possibility of integrating nanogap field emitters into the standard complementary metal oxide semiconductor electronic devices and the potential of vacuum nanoelectronics in low-power consumption devices.

For samples with 60 and 80 nm gaps, the current at the same applied voltage is much lower than that for emitters with 20 and 40 nm gaps and no obvious linear behaviour has been observed in the corresponding F–N plot. Therefore it can be concluded that no significant field emission current has been measured for emitters with 60 and 80 nm gaps. Fig. 3 shows a strong dependence of field emission current on the cathode–anode distance, which has potential use in nanometre scale sensing.

Table 1 Performance comparison of emitters with small gaps. Here r is the radius of the emitter

Tip material	Tip amount	r/nm	Electrode gap	V_{on}/V	Vacuum/para
tungsten [29]	single	18	1 mm	~ 800	5×10^{-8}
silicon [28]	single	–	75 nm	~ 45	$\sim 1 \times 10^{-4}$
carbon nanotube [30]	single	7.5	2.65 μm	115	in SEM
Ti [31]	multiple	–	20 μm	2	$\sim 1 \times 10^{-5}$
SiC [32]	single	40	20 nm	3.2	$\sim 1 \times 10^{-3}$
Cu (this work)	single	~ 20	~ 20 nm	1.75	Air

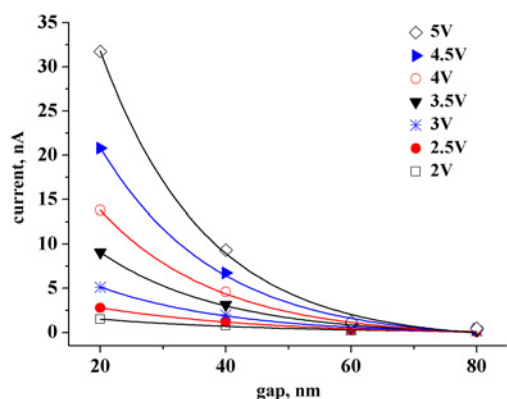


Fig. 3 Emission current at a fixed voltage decreases exponentially with the increase of electrode gap

For emitters with 20 and 40 nm gaps, the field enhancement factors calculated from the slope of F–N plots are ~ 250.8 and ~ 594.0 , respectively. These values are much lower than those reported for field emitters with microgaps (10^3 – 10^5) [9, 24–27] indicating the deterioration of field enhancement with the decrease in the cathode–anode gap. This reduction in the field enhancement factor has been previously reported for a 75 nm gap and attributed to the quantum screening effect [28]. In this effect, the increased potential barrier in the nanogap impedes the electron F–N tunnelling so that field enhancement factors observed in field emission experiments with nanoscale gaps are usually lower than that with microgaps. Due to the quantum screening effect, the electron tunnelling is much more reduced for 20 nm gaps with a result of a lower field enhancement factor than that for 40 nm. In previous work, the

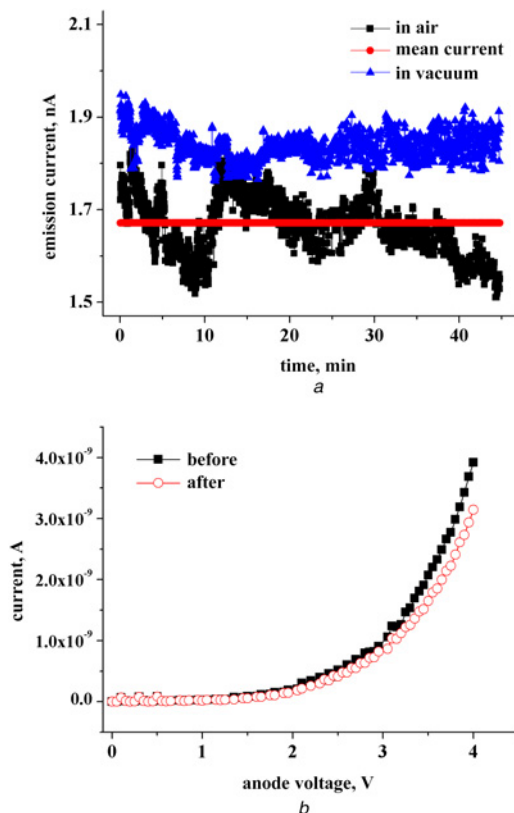


Fig. 4 Field emission stability measurement
a Field emission stability of a single Cu emitter with a 40 nm gap at 3 V in air and vacuum for 45 min
b Field emission properties before and after the stability measurement in air

quantum screening effect has only been reported for the emitter and anode made of different materials, therefore the work function difference between the emitter and anode is suspected to play a role. However, the quantum screening effect is observed here for the emitter and anode from the same Cu nanowire with no work function difference. Although the turn-on voltage (to induce 1 nA) for 20 nm gap samples which is 1.75 V is smaller than that for 40 nm gap samples (2.25 V), the turn-on applied electric field for 20 nm gap samples is higher, which also indicates a deterioration of field emission efficiency.

In addition, the emission current at a fixed voltage decreases exponentially with the increase in the electrode gap and the exponential fitting corresponds well with the experimental data as depicted in Fig. 3. No saturation of emission current is observed as the gap is scaled from 80 to 20 nm, which indicates the possibility of scaling for field emission-based devices such as VFETs in the nanoscale.

The stability of a single Cu emitter with a 40 nm gap was measured in air with 3 V applied voltage. Several fluctuations are observed for 45 min as shown in Fig. 4*a*. After the stability test, an anode voltage from 0 to 4 V was applied which resulted in 20% attenuation in the emission current (Fig. 4*b*). The electron energy loss spectroscopy analysis in transmission electron microscopy (TEM) did not show sufficient oxygen for the oxidation of the copper tip, so the copper emitter remains to be metal instead of metallic oxide during the field emission measurement. The fluctuations and attenuation can be from the degeneration of emitters caused by Joule heating or from the absorption/desorption process of gas molecules at the tips. As TEM images show no significant differences between the emitter before and after the stability test (Fig. 5), the gas molecules in air may be responsible for the fluctuations and attenuation during our stability test. Moderate

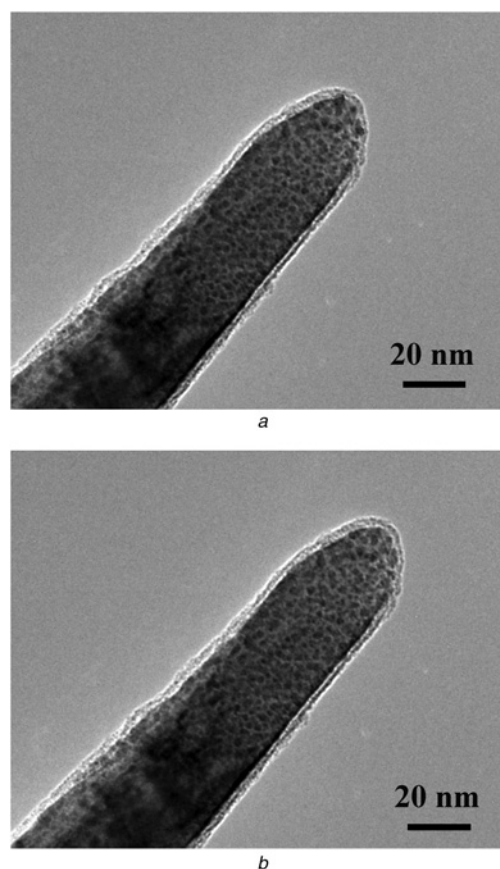


Fig. 5 TEM images
a Before the 45 min field emission stability test in air
b After the 45 min field emission stability test in air

vacuum packaging as in microelectromechanical systems may alleviate this problem. To validate it, a similar field emission stability measurement was carried out in a Lake Shore Cryotronics Probe Station with a vacuum of $\sim 1 \times 10^{-3}$ Pa. The emission in vacuum is much more stable than that in air with a higher current at the same voltage as presented in Fig. 4a, indicating that the reduction of the amount of air molecules can effectively improve the field emission performance from emitters with 40 nm gaps.

4. Conclusion: Nanoscale emitter-collector gaps were created in a controlled manner using FIB to study the emission characteristics of copper emitters. Cu, W and similar metals may be an alternative to silicon emitters in VFETs [1–4]. Since the electrode gaps in this study are smaller than the electron mean free path in air, the need for vacuum was relaxed and emission was achieved under ambient conditions. This result has certain economic significance by lowering the package cost and simplifying the structure of vacuum electronics. The field emission turned on at around 1.75 V and the emission current increased to 32.5 nA at 5 V for the smallest gap of 20 nm here. These values represent the lowest voltage operation and the highest current for the smallest electrode gaps to date in the literature. The emission current is dependent on the cathode–anode gap as expected and increases exponentially at a constant voltage with a decrease in the electrode gap. While an increase in frequency and current at fixed V_{ds} with a decreasing channel length is well known and taken for granted for MOSFET, the same cannot be said for vacuum devices. No one knows yet if the current of vacuum devices with such small gaps will be influenced by any ‘quantum screening’. Our experimental results from 80 to 20 nm gap show no current saturation, which indicates the potential absence of ‘quantum screening’ in current for a given drive voltage with reduced gaps at the nanoscale. The emission shows instability and a reduction in current after some time possibly due to molecular absorption, and future work should include careful vacuum studies to address the issue and mechanisms. The present results help to understand the field emission mechanism of emitters with nanogaps, which is valuable for the future development of vacuum nanoelectronics including VFETs.

5. Acknowledgments: This work was supported by the National Basic Research Program of China (grant no. 2012CB933300), the Fund for Creative Research of the National Natural Science Foundation of China (grant no. 61321492) and the Project of the National Natural Science Foundation of China (grant no. 61327811). The author of this article assumes responsibility for its content and would like to thank the team for the support.

6 References

[1] Han J.-W., Sub Oh J., Meyyappan M.: ‘Vacuum nanoelectronics: back to the future? Gate insulated nanoscale vacuum channel transistor’, *Appl. Phys. Lett.*, 2012, **100**, p. 213505

[2] Jin-Woo H., Jae Sub O., Meyyappan M.: ‘Cofabrication of vacuum field emission transistor (VFET) and MOSFET’, *IEEE Trans. Nanotechnol.*, 2014, **13**, pp. 464–468

[3] Subramanian K., Weng Poo K., Davidson J.L.: ‘A monolithic nanodiamond lateral field emission vacuum transistor’, *IEEE Electron Device Lett.*, 2008, **29**, pp. 1259–1261

[4] Park I.J., Jeon S.G., Shin C.: ‘A new slit-type vacuum-channel transistor’, *IEEE Trans. Electron Devices*, 2014, **61**, pp. 4186–4191

[5] Kim J., Kim J., Oh H., *ET AL.*: ‘Design guidelines for nanoscale vacuum field emission transistors’, *J. Vacuum Sci. Technol. B*, 2016, **34**, p. 042201

[6] Han J.W., Moon D.I., Meyyappan M.: ‘Nanoscale vacuum channel transistor’. *IEEE Int. Conf. on Nanotechnology*, 2017, pp. 172–175

[7] Shin D.H., Jung S.I., Yun K.N., *ET AL.*: ‘Field emission properties from flexible field emitters using carbon nanotube film’, *Appl. Phys. Lett.*, 2014, **105**, p. 033110

[8] Dimitrijevic S., Withers J.C., Mammana V.P., *ET AL.*: ‘Electron emission from films of carbon nanotubes and ta-C coated nanotubes’, *Appl. Phys. Lett.*, 1999, **75**, pp. 2680–2682

[9] Yeong K.S., Thong J.T.L.: ‘Field-emission properties of ultrathin 5 nm tungsten nanowire’, *J. Appl. Phys.*, 2006, **100**, p. 114325

[10] Spindt C.A.: ‘A thin-film field-emission cathode’, *J. Appl. Phys.*, 1968, **39**, pp. 3504–3505

[11] Geis M.W., Twichell J.C., Lyszczarz T.M.: ‘Diamond emitters fabrication and theory’, *J. Vac. Sci. Technol. B, Microelectron. Nanometer Struct.*, 1996, **14**, pp. 2060–2067

[12] Thomas R.N., Wickstrom R.A., Schroder D.K., *ET AL.*: ‘Fabrication and some applications of large-area silicon field emission arrays’, *Solid State Electron.*, 1974, **17**, p. 155

[13] Xu Z., Bai X.D., Wang E.G.: ‘Geometrical enhancement of field emission of individual nanotubes studied by in situ transmission electron microscopy’, *Appl. Phys. Lett.*, 2006, **88**, p. 133107, IN1–163, IN7

[14] Hii K.F., Vallance R.R., Chikkamarahalli S.B., *ET AL.*: ‘Characterizing field emission from individual carbon nanotubes at small distances’, *J. Vac. Sci. Technol. B, Microelectron. Nanometer Struct.*, 2006, **24**, pp. 1081–1087

[15] Liu H., Kato S., Saito Y.: ‘Effect of cathode–anode distance on field emission properties for carbon nanotube film emitters’, *Jpn. J. Appl. Phys.*, 2009, **48**, pp. 29–33

[16] Kumar S., Duesberg G.S., Pratap R., *ET AL.*: ‘Graphene field emission devices’, *Appl. Phys. Lett.*, 2014, **105**, p. 103107

[17] Dong C.L., Ahn H.S., Choi D.J., *ET AL.*: ‘The field emission properties of silicon carbide whiskers grown by CVD’, *Surf. Coat. Technol.*, 2003, **168**, pp. 37–42

[18] Wang L., Gao F., Chen S., *ET AL.*: ‘Nanowire-density-dependent field emission of n-type 3C-SiC nanoarrays’, *Appl. Phys. Lett.*, 2015, **107**, p. 122108

[19] Chen S., Ying P., Wang L., *ET AL.*: ‘Temperature-dependent field emission of flexible n-type silicon carbide nanoneedle emitters’, *Appl. Phys. Lett.*, 2014, **105**, p. 133106

[20] Hsu S.H., Kang W.P., Davidson J.L., *ET AL.*: ‘Performance characteristics of nanocrystalline diamond vacuum field emission transistor array’, *J. Appl. Phys.*, 2012, **111**, p. 114502

[21] Hsu S.H., Kang W.P., Wisitsora-at A., *ET AL.*: ‘Nitrogen-incorporated nanodiamond vacuum field emission transistor with vertically configured self-aligning gate’, *Diam. Relat. Mater.*, 2012, **22**, pp. 142–146

[22] Xu Z., Bai X.D., Wang E.G.: ‘Geometrical enhancement of field emission of individual nanotubes studied by in situ transmission electron microscopy’, *Appl. Phys. Lett.*, 2006, **88**, pp. 133107–133107-3

[23] Zhang D., Wang R., Wen M., *ET AL.*: ‘Synthesis of ultralong copper nanowires for high-performance transparent electrodes’, *J. Am. Chem. Soc.*, 2012, **134**, p. 14283

[24] Shang D., Ke Y., Zhang Y., *ET AL.*: ‘Magnetic and field emission properties of straw-like CuO nanostructures’, *Appl. Surf. Sci.*, 2009, **255**, pp. 4093–4096

[25] Tang C.-C., Xu X.-W., Hu L., *ET AL.*: ‘Improving field emission properties of GaN nanowires by oxide coating’, *Appl. Phys. Lett.*, 2009, **94**, p. 243105

[26] Yu W., Hu H., Zhang D., *ET AL.*: ‘Improved field emission properties of CuO nanowire arrays by coating of graphene oxide layers’ (Editions en Langues Etrangères, 2016)

[27] Li M., Kong F., Li L., *ET AL.*: ‘Synthesis, field-emission and electric properties of metastable phase VO₂ (A) ultra-long nanobelts’, *Dalton Trans.*, 2011, **40**, p. 10961

[28] Cheng T.C., Chen P.Y., Wu S.Y.: ‘Paradox of low field enhancement factor for field emission nanodiodes in relation to quantum screening effects’, *Nanoscale Res. Lett.*, 2012, **7**, p. 125

[29] Yamada T.K., Abe T., Nazriq N.M.K., *ET AL.*: ‘Electron-bombarded (110)-oriented tungsten tips for stable tunneling electron emission’, *Rev. Sci. Instrum.*, 2016, **87**, p. 033703

[30] Bonard J.M., Dean K.A., Coll B.F., *ET AL.*: ‘Field emission of individual carbon nanotubes in the scanning electron microscope’, *Phys. Rev. Lett.*, 2002, **89**, p. 197602

[31] Pennisi S., Castorina G., Patti D.: ‘Dovetail tip: a new approach for low-threshold vacuum nanoelectronics’, *IEEE Trans. Electron Devices*, 2015, **62**, pp. 4293–4300

[32] Liu M., Li T., Wang Y.: ‘SiC emitters for nanoscale vacuum electronics: a systematic study of cathode–anode gap by focused ion beam etching’, *J. Vac. Sci. Technol. B, Microelectron. Nanometer Struct.*, 2017, **35**, p. 031801